



Oxygen segregation in pre-hydrided Zircaloy-4 cladding during a simulated LOCA transient

Elodie Torres, Jean Desquines, Severine Guilbert, Pauline Lacote,
Marie-Christine Baietto, Michel Coret, Martine Blat, Antoine Ambard

► To cite this version:

Elodie Torres, Jean Desquines, Severine Guilbert, Pauline Lacote, Marie-Christine Baietto, et al..
Oxygen segregation in pre-hydrided Zircaloy-4 cladding during a simulated LOCA transient. EPJ N
- Nuclear Sciences & Technologies, 2017, 3, 10.1051/epjn/2017020 . hal-01951563

HAL Id: hal-01951563

<https://hal.science/hal-01951563>

Submitted on 12 Dec 2018

HAL is a multi-disciplinary open access archive for the deposit and dissemination of scientific research documents, whether they are published or not. The documents may come from teaching and research institutions in France or abroad, or from public or private research centers.

L'archive ouverte pluridisciplinaire **HAL**, est destinée au dépôt et à la diffusion de documents scientifiques de niveau recherche, publiés ou non, émanant des établissements d'enseignement et de recherche français ou étrangers, des laboratoires publics ou privés.



Distributed under a Creative Commons Attribution 4.0 International License

OXYGEN SEGREGATION IN PRE-HYDRIDED ZIRCALOY-4 CLADDING DURING A SIMULATED LOCA TRANSIENT

E. TORRES, J. DESQUINES, S. GUILBERT, P. LACOTE

*Institut de Radioprotection et de Sûreté Nucléaire (IRSN), Centre d'Etudes de Cadarache,
PSN-RES/SEREX/LE2M
BP3, 13115 Saint Paul-Lez-Durance cedex – France*

M.-C. BAIETTO

*INSA de Lyon, Laboratoire de Mécanique des Contacts et des Structures (LaMCoS), UMR 5259
69621 Villeurbanne cedex – France*

M. CORET

*École Centrale de Nantes, Institut de recherche en génie civil et mécanique (GEM), UMR 6183
44321 Nantes – France*

M. BLAT, A. AMBARD

*EDF-R&D, Les Renardières, département MMC
77818 Moret sur Loing - France*

ABSTRACT

Oxygen and hydrogen distributions are key elements influencing the residual ductility of zirconium-based nuclear fuel cladding during the quench phase following a Loss Of Coolant Accident (LOCA). During the high temperature oxidation, a complex partitioning of the alloying elements is observed. A finite-difference code for solving the oxygen diffusion equations has been developed by IRSN to predict the oxygen profile within the samples. The comparison between the calculations and the experimental results in the mixed $\alpha+\beta$ region shows that the oxygen diffusion is not accurately predicted by the existing modeling. This work aims at determining the key parameters controlling the average oxygen profile within the sample in the two-phase regions at 1200°C. High temperature steam oxidation tests interrupted by water quench were performed using pre-hydrided Zircaloy-4 samples. Experimental oxygen distribution was measured by Electron Probe Micro-Analysis (EPMA). The phase distributions within the cladding thickness, was measured using image analysis to determine the radial profile of $\alpha(O)$ phase fraction. It is further demonstrated and experimentally checked that the α -phase fraction in these regions follows a diffusion-like radial profile. A new phase fraction modeling is then proposed in the cladding metallic part during steam oxidation. The modeling results are compared to a large set of experiments including the influence of exposure duration and hydrogen content. Another key outcome from this modeling is that oxygen average profile is straightforward derived from the proposed modeling.

1. Introduction

During a Loss Of Coolant Accident, zirconium-based nuclear fuel claddings are submitted to high temperature steam oxidation before core reflooding. During the high temperature oxidation, metallurgical evolutions due to α - β phase transformations are observed in the material (

Fig. 1). A partitioning of the main chemical elements is also evidenced within the cladding thickness. This segregation is associated to oxygen diffusion and progressive transformation of the β -phase into an oxygen stabilized $\alpha(O)$ layer. The microstructure results in a complex distribution of oxygen and hydrogen in the two-phase constituted material.

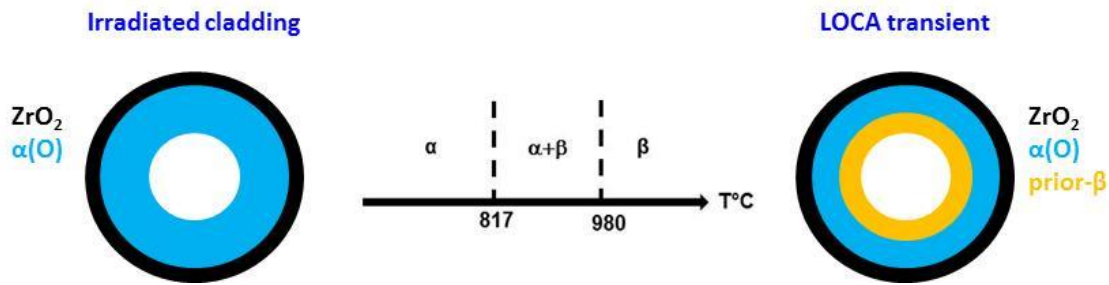


Fig. 1. Metallurgical evolutions of Zircaloy-4 alloy during a LOCA transient [1]

These phenomena have a direct impact on the material mechanical properties [2]. It was frequently reported that oxygen and hydrogen contents in the prior- β phase or in the $\alpha+\beta$ phase had a combined influence on the cladding post quenching embrittlement [2-7]. It is thus necessary to understand the mechanisms influencing the motion of these two chemical elements to fully describe the post-quench embrittlement.

Hydrogen distribution within the cladding was previously discussed in another paper [8]. In the open literature, analytical oxygen diffusion models are restricted to samples having simple geometry that is usually not satisfactory to analyze tubular geometry [9]. A finite-difference software solving the oxygen diffusion equations named DIFFOX has been developed by IRSN [10]. The comparison between the calculations and the experimental results in the mixed $\alpha+\beta$ region shows that the oxygen diffusion is not accurately predicted. This work aims at determining experimentally the key parameters controlling the average oxygen profile within the sample both in the prior- β phase and the $\alpha+\beta$ region at 1200°C. This study provides improved modeling to be implemented in the diffusion softwares.

Several Zircaloy-4 samples are pre-hydrided with hydrogen contents ranging between the as-received content (~ 10 wppm) and 400 wppm. The samples are then steam oxidized at high temperature (1200°C), to simulate LOCA conditions, and then quenched in a water bath at room temperature. The microstructure of the material, especially the phase distributions within the cladding thickness, is systematically characterized by metallography. Local oxygen concentrations are specifically investigated using Electron Probe Micro-Analysis (EPMA). Experimental radial oxygen distributions can then be compared to several diffusion modeling results.

This paper describes the test devices and the experimental method supporting this study. The experimental results are presented, discussed and compared to those predicted numerically using calculations derived from the DIFFOX tool. A new modeling is thus proposed. The improved modeling is then validated by comparison to a large set of experiments including influence of exposure duration and hydrogen content.

2. Materials and method

2.1 Materials

The specimens investigated in this study are stress-relieved annealed low tin Zircaloy-4 fuel cladding tubes provided by AREVA-NP. The tubular samples are 70 mm long, have a 9.5 mm outer diameter and a 570 μm thickness respectively. Chemical composition of the tested material is detailed in Table 1.

Table 1. Chemical composition of the tested Zircaloy-4

Sn (wt%)	Fe (wt %)	Cr (wt %)	O (wt %)	H (wppm)	Zr
1.3	0.21	0.10	0.13	10	balance

2.2 Experiments

The 70 mm long specimens are first pre-hydrided at the École Centrale de Paris using gaseous charging at 420°C. More details about hydrogen gaseous charging are provided in a previous paper [11]. The tubes are then cut into 20 mm long segments for oxidation and thin ring samples both for hydrogen measurements and for metallographic analyses before oxidation. Two-sided steam oxidations are then performed in a vertical furnace at 1200°C in a mixture of argon and steam. The argon and steam flow rates are respectively 10NL.min⁻¹ and 500g.h⁻¹ (50 vol% argon and 50 vol% steam) in order to prevent steam starvation and limit hydrogen pick-up. Oxidation durations are adjusted to reach ECR (Equivalent Clad Reacted) values of 15%, 20% and 25% using Cathcart-Pawel correlation assuming inner and outer diameter oxidation [12]. Oxidation is interrupted by dropping the sample into a water bath at room temperature as illustrated in Fig.2. More details about the oxidation protocol and its qualification are provided by Duriez and Guilbert [10, 13, 14].

Radial cross sections are prepared for hydrogen measurements and microstructure analyses. Oxygen profiles are systematically measured using EPMA on each radial cut. The microstructure of the material, especially the phase distributions within the cladding thickness, is characterized by metallography.

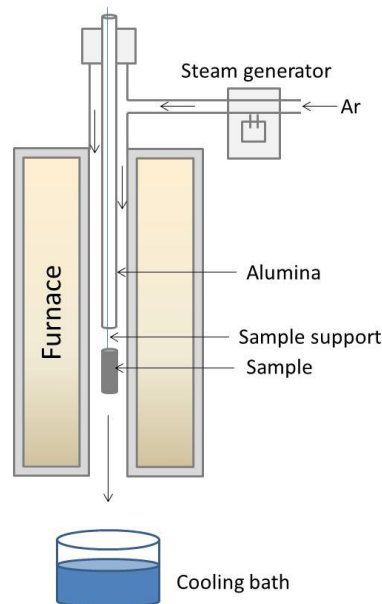


Fig. 2. Vertical furnace used for the steam oxidations at 1200°C.

2.3 Samples characterizations

Hydrogen measurements

The hydrogen content of the samples is measured using a Brücker ONH mat 286 by melting the sample at 2000°C in the presence of a carrier gas (argon). After calibration, the hydrogen content is determined by catharometry comparing the conductivity of the mixture with the one of pure argon. For 70 mm long tube samples, four axial locations are systematically investigated. A minimum of four analyses at each axial location are performed to check the homogeneity of hydrogen content. After measurement, the zirconia is partially melted in the graphite crucible. Brachet and Rapsaet have shown by ERDA measurements that the hydrogen content is negligible in the zirconia layer after oxidation at high temperature [15, 16]. The zirconia layer weight is thus subtracted to take into account the melted sample weight. Hydrogen is measured after gaseous charging and after steam oxidation.

Metallurgical examinations

After oxidation, two metallographic radial cross sections are cut at each end for all the tested samples. Metallurgical examinations are performed to determine the various material layers thicknesses obtained after the LOCA transient. Oxygen diffusion profiles are investigated by Electron Probe Micro Analysis (EPMA) using a CAMECA SX100 electron probe. Each radial cross section of the samples is embedded in a conductive resin along with an as-received Zircaloy-4 sample. After mechanical polishing, a chemical etching with a fluorhydric acid solution is performed before introduction into the microprobe vacuum chamber. Oxygen $K\alpha$ line is measured with a W/Si multi-layer synthetic crystal. Oxygen calibration is performed using as-received Zircaloy-4 with homogeneous and well known oxygen contents. A typical accuracy of 0.2 wt% is expected for oxygen content measurements. All the profiles are measured across the thickness with 1 μm stage displacement step in each phase and 250 nm stage displacement step at the zirconia/ $\alpha(\text{O})$ and $\alpha(\text{prior-}\beta)$ interfaces. Point analyses are also performed in the $\alpha(\text{O})$ inclusions, the $\alpha(\text{O})$ layer and in the prior- β phase. Maps are obtained from 400x300 μm^2 areas with a stage displacement step of 1 μm during 300 ms per point.

Optical microscopy was used to measure the oxide and $\alpha(\text{O})$ layers thickness. The phase distribution in the metallic part of the samples is determined by image analysis based on a half ring metallography reconstruction. The metallography is first transformed into a binary image representing each of the two phases in the metal (Fig. 3). This binary image is then used to determine the average radial profile of $\alpha(\text{O})$ phase fraction $f(\alpha)$.

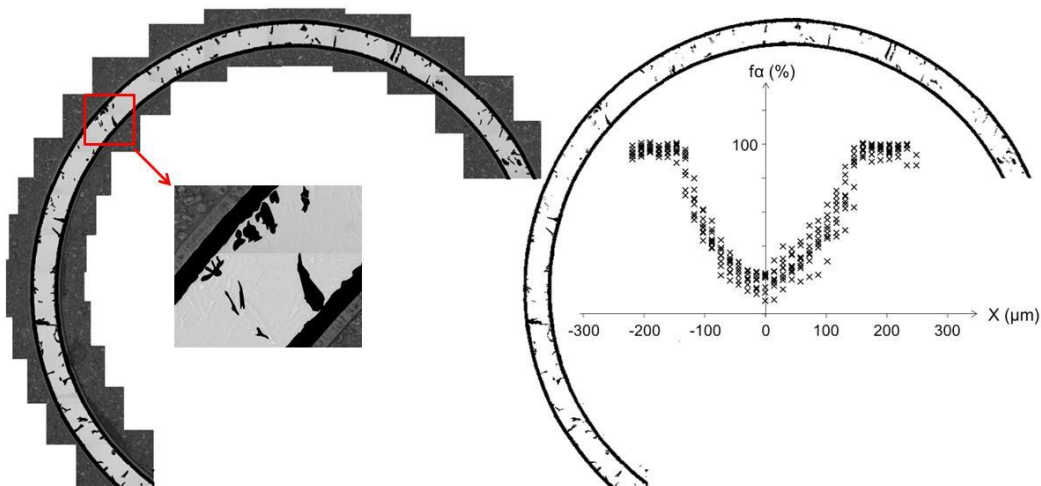


Fig. 3. Example of transformation of the optical metallography into a binary image used to determine the experimental average phase fraction radial profile (sample labelled H66-7).

3. Results and discussion

3.1 Oxidation results

The typical microstructure of Zircaloy-4 samples after steam oxidation at 1200°C is illustrated in Fig. 4. The measured values of some parameters such as the measured Equivalent Clad Reacted (ECR), initial and final hydrogen contents, $\alpha(\text{O})$ and zirconia layer thicknesses are respectively reported in Table 2. The results indicate low hydrogen pickup during oxidation. A good consistency between measured ECR and its assessment using Cathcart-Pawel correlation is obtained [12]. No influence of hydrogen content on the measured ECR is observed. Hydrogen has no effect on the oxide and oxygen stabilized layer growth. All the results are in agreement with the literature data [2, 13, 17].

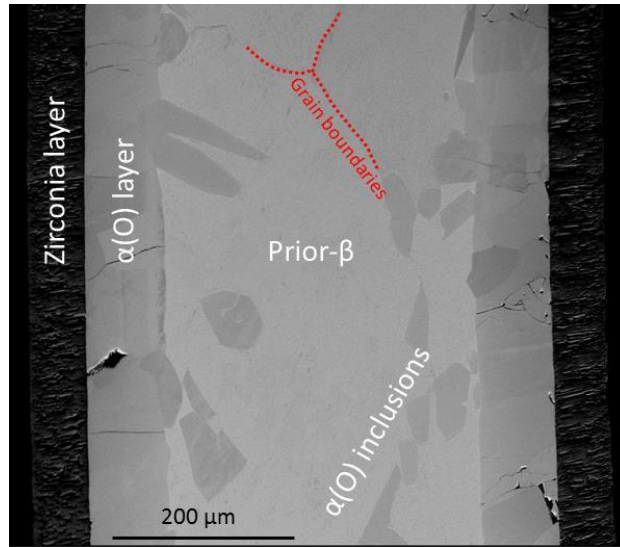


Fig. 4. SEM micrograph of Zircaloy-4 after oxidation at 1200°C during 400s (H60-5)

Table 2. Oxidation results

Sample	Time	Initial hydrogen content	final hydrogen content	ZrO ₂ layer thickness	α(O) layer thickness	Measured ECR	α(O) phase fraction
(#)	s	wppm	wppm	μm	μm	%	%
AR-1	624	11 ± 5	18 ± 2	71	92	23.6	66
AR-2	400	11 ± 5	15 ± 2	58	79	19.6	-
AR-3	196	11 ± 5	15 ± 2	44	59	14.7	-
H64-3	624	144 ± 17	214 ± 19	74	96	24.2	76
H64-5	400	147 ± 17	210 ± 20	59	81	20.2	58
H64-7	196	173 ± 24	219 ± 26	44	59	14.9	32
H60-3	624	305 ± 39	396 ± 35	72	100	23.8	62
H60-5	400	287 ± 32	376 ± 34	58	80	19.0	51
H60-7	196	305 ± 38	356 ± 34	42	59	14.1	27
H66-3	624	92 ± 12	116 ± 10	74	104	23.9	79
H66-5	400	86 ± 9	114 ± 11	57	82	19.8	61
H66-7	196	92 ± 12	104 ± 11	43	58	14.3	45
H58-3	624	149 ± 17	199 ± 17	68	92	23.8	67
H58-5	400	157 ± 18	202 ± 18	58	78	19.7	51
H58-7	196	165 ± 18	191 ± 18	43	59	15.1	30

3.2 Oxygen distribution

Oxygen partitioning occurs within the thickness of the cladding tube during the high temperature oxidation. This segregation results from oxygen diffusion inducing a progressive transformation of the β phase into an oxygen stabilized $\alpha(O)$ layer [18, 19]. Oxygen segregation within the cladding samples is systematically analyzed using EPMA. Typical oxygen concentration using point measurements or mapping are illustrated in Fig. 5.

Oxygen is segregated into the α -phase consistently with its α -stabilizing properties. Oxygen concentrations are accurately determined by point analysis in each phase. The electron beam is defocused to obtain a lower sensitivity to short range discrepancies. About 10 measurement points per phase are acquired. Results are plotted in Fig. 5(b).

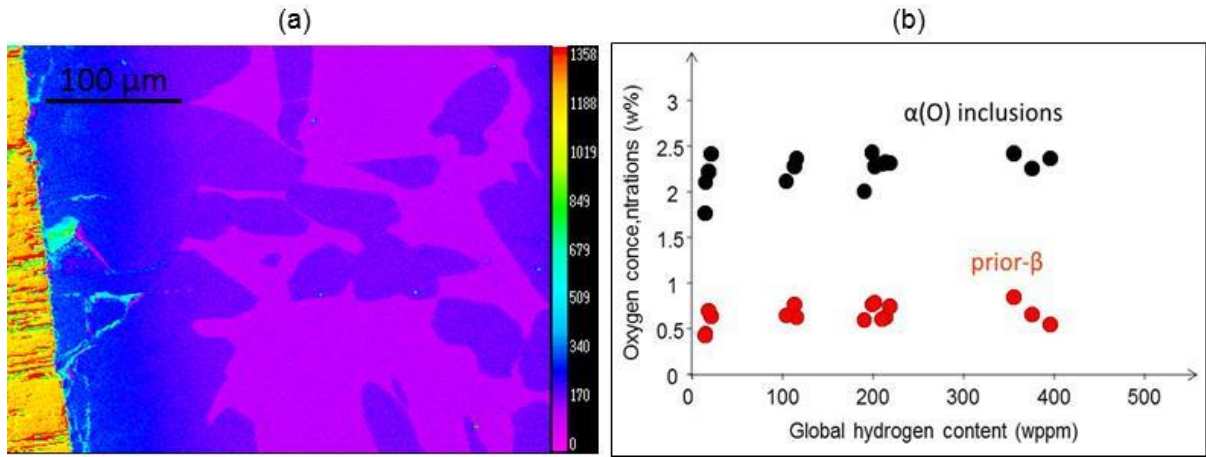


Fig. 5. Oxygen measurements obtained by EPMA of Zircaloy-4 after oxidation at 1200°C
 (a) Maps in the wall cladding (H64-3) and (b) oxygen concentrations in each phase

3.3 Oxygen concentration profiles modeling

DIFFOX is a 1D finite-difference calculation code describing several connected reaction layers used to solve the oxygen diffusion equations. It has been developed by IRSN to address LOCA induced oxidation [10]. The oxygen concentration profile is calculated by solving the 2nd Fick Law diffusion equation in cylindrical coordinates according to Eq. 1. The left side is considered to be the oxygen accumulation and the right side the space change of the diffusion flux F_r . The oxygen flux is assumed to be proportional to the oxygen gradient according to the 1st Fick Law (Eq. 2). The motion of layer boundaries is derived from the mass balance of oxygen at the interface between two layers according to Stefan equation (Eq. 3). The oxygen diffusion coefficient is extracted from literature data for each of the α(O) phase and β-phase. Considering now the mixed α+β phase, it is assumed that the oxygen motion is described by a diffusion law applicant to the average oxygen content. Nevertheless, the equivalent diffusion coefficient has to be determined. In the DIFFOX code, this diffusion coefficient was empirically determined as well as the conditions required to form a layer containing mixed α+β phases.

$$\frac{\partial C(r,t)}{\partial t} = \frac{1}{r} \times \frac{\partial}{\partial r} (r \cdot F_r) \quad (\text{Eq.1})$$

$$F_r = -D_i(T) \frac{\partial C(r,t)}{\partial r} \quad (\text{Eq. 2})$$

Where $C(r,t)$ is the oxygen concentration, $D_i(T)$ is the oxygen diffusion coefficient in phase i ($i=\alpha, \beta, \alpha+\beta$), t is the time and r is the radius.

$$\frac{\partial S}{\partial t} = \frac{F_+ - F_-}{2\pi S(C_+ - C_-)} \quad (\text{Eq. 3})$$

Where S is the interface radius, F_+ and F_- are the left and right side oxygen fluxes, C_+ and C_- the oxygen concentrations at each side of the interface.

Measured oxygen distributions are compared to DIFFOX predictions in Fig.6. The calculations accurately determine the α-layer thickness but strongly underestimate the oxygen content within the α(O) inclusions in the α(O)+β regions. EPMA indicates that in the α(O) inclusions and in the prior-β phase, the oxygen content is constant but different in each

of the two phases. Consequently, the equivalent averaged oxygen radial profile can be determined using the $\alpha(\text{O})$ -phase radial profile. The measurement of oxygen average profile combining EPMA determined concentrations in each phase and average phase radial profile are summarized in Eq. 4.

$$[O] = C_{\alpha}^0 \cdot f_{\alpha} + C_{\beta}^0 \cdot f_{\beta} \quad (\text{Eq. 4})$$

A rather continuous oxygen profile is obtained between the $\alpha(\text{O})$ layer and the two-phase region. Experimental and calculated profiles are illustrated in Fig.6.

The comparison between the calculations and measurements in the mixed $\alpha+\beta$ region shows that the oxygen diffusion is not accurately predicted by the modeling tools.

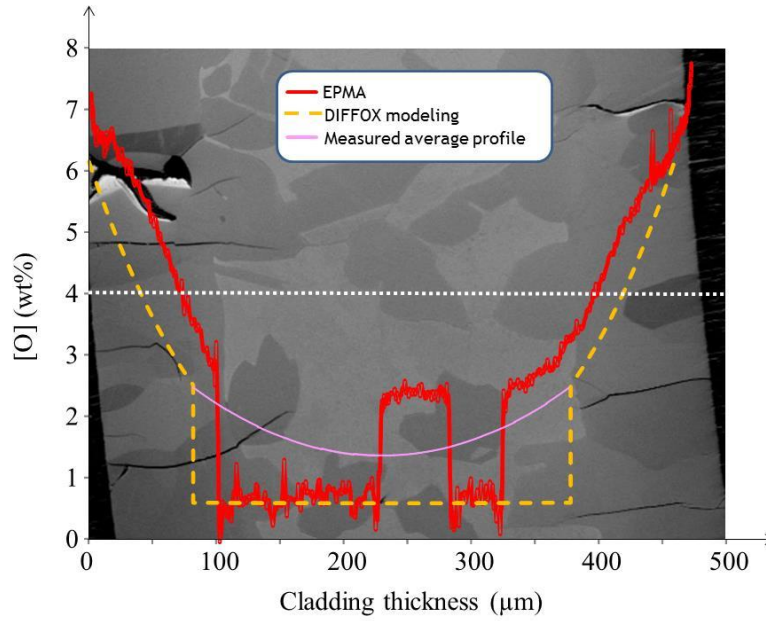


Fig. 6. EPMA oxygen profiles versus Difffox calculation or measured average profile (H64-3)

3.4 Oxygen distribution in the two-phase region

Assuming that the oxygen diffusion in the $\alpha+\beta$ phase is governed by the 2nd Fick type law, the combined Eq. 1 and Eq. 4 implies that α -phase fraction is also governed by a diffusion-like law having the same diffusion coefficient (Eq. 5).

$$\frac{df_{\alpha}}{dt} = D_{\alpha+\beta} \frac{\partial^2 f_{\alpha}}{\partial r^2} \quad (\text{Eq. 5})$$

If the phase fraction is governed by a diffusive process, it is also interesting to consider that Eq.5 implies that oxygen distribution follows an Eq. 1 diffusion type law.

Two types of input data are thus needed for the new calculations: the equilibrium concentration at each interface and the diffusion coefficient in the two-phase region. The oxygen concentrations are relying on EPMA measurements illustrated in Fig. 5(b).

A Crank analytical solution [20] is first used to determine the concentration profile between the edges of a thick plate having constant concentration at each edge ($r = \pm l$). This solution is used to describe the phase fraction in a cladding having only an $\alpha+\beta$ region layered by

$\alpha(O)$. Indeed, this situation corresponds to long steam exposure at elevated temperature with no remaining β -phase in the central region of the cladding. The boundary layer condition is determined assuming continuity with $\alpha(O)$ uniform layer ($f_\alpha(\pm l, t) = 1$) at the edges of $\alpha+\beta$ region. The proposed solution is assumed to be acceptably good close to the $\alpha/\alpha+\beta$ interface and accurate enough for a first order assessment of the oxygen diffusion coefficient $D_{\alpha+\beta}$. The Crank analytical solution [20] is given by Eq. 6. The diffusion coefficient $D_{\alpha+\beta}$ is adjusted in the solution to fit measured phase fraction profile with the proposed analytical solution.

$$f_{\alpha}(r,t) = \frac{4}{\pi} \sum_{n \geq 0} \left[\frac{(-1)^n}{(2n+1)} \exp\left(-\frac{D_{\alpha+\beta}(2n+1)^2 \pi^2 t}{4l^2}\right) \cos\left(\frac{(2n+1)\pi r}{2l}\right) \right] \quad (\text{Eq. 6})$$

A diffusion coefficient $D_{\alpha+\beta}$ equal to $1.5 \cdot 10^{-7} \text{ cm}^2/\text{s}$ was obtained when simulating the measured radial distribution of phase fraction. The obtained diffusion coefficient was poorly dependent on sample average hydrogen content suggesting that the oxygen diffusion is not influenced by hydrogen.

A new model is developed including a moving interface satisfying the following conditions:

- If the oxygen concentration is less than the solubility limit in the β -phase, the $\alpha(O)$ -phase fraction is equal to zero. Oxygen diffusion is thus homogeneous in this phase and governed by Eq. 7 with D_β is equal to $1.6 \cdot 10^{-6} \text{ cm}^2/\text{s}$ [21].

$$\frac{d[o]}{dt} = D_\beta \frac{\partial^2 [o]}{\partial r^2} \quad (\text{Eq.7})$$

- If the oxygen concentration in the β -phase reaches the solubility limit, the phase fraction increases at the considered location and follows Eq.8. In this situation, the oxygen concentration in both the $\alpha(O)$ inclusions and the prior- β phase are determined relying on EPMA measurements (Fig.5). The link between phase fraction and oxygen content is established by Eq. 4. The inclusion growth is then controlled by grain boundary diffusion of oxygen along the $\alpha(O)$ inclusion interface with β -phase as described by Eq. 8 where $D_{\alpha+\beta}$ is an empirical overall diffusion coefficient for the two-phases layer.

$$\frac{df_\alpha}{dt} = D_{\alpha+\beta} \frac{\partial^2 f_\alpha}{\partial r^2} \quad (\text{Eq.8})$$

In other words, the oxygen diffusion follows $\frac{d[o]}{dt} = D_{\alpha+\beta} \frac{\partial^2 [o]}{\partial r^2}$ diffusion equation.

- The $\alpha/\alpha+\beta$ interface motion is governed by Eq.9 using experimental measurements for both $\alpha(O)$ and zirconia layer thicknesses.

$$r_{\text{interface}} = \alpha(O)_{\text{measured}} + \frac{1}{1,56} e_{\text{zirconia}} (\text{measured}) \quad (\text{Eq.9})$$

and $f_\alpha(r_{\text{interface}}, t) = 1$

A good consistency between the average phases fractions measured across the sample metallic surfaces versus oxidation time is obtained for a $D_{\alpha+\beta}$ value of $1.5 \cdot 10^{-7} \text{ cm}^2/\text{s}$ as illustrated in Fig. 7. Experiments obtained in this study but also from previous experiments conducted at IRSN with identical material are then simulated in order to validate this approach in the $\alpha+\beta$ regions. A good consistency is obtained between measured and predicted $\alpha(O)$ -phase fraction as illustrated in Fig. 8.

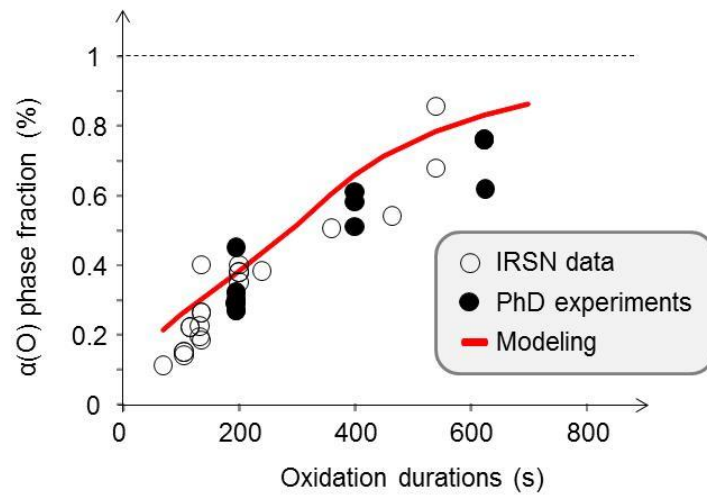


Fig. 7. Measured $\alpha(O)$ average phase fraction versus modeling using numerically determined oxygen diffusion coefficient in the $\alpha+\beta$ region

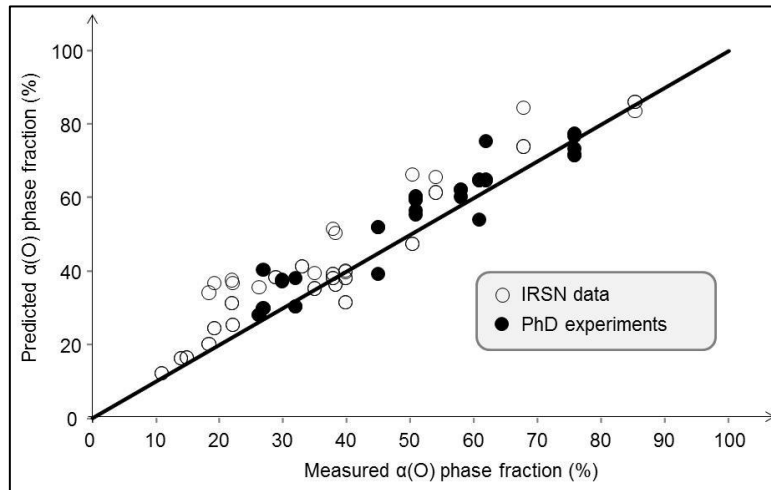


Fig. 8. Comparison between predicted and measured $\alpha(O)$ phase fraction

4. Conclusions and perspectives

The present study addresses oxygen distribution in Zircaloy-4 cladding after a LOCA steam oxidation transient. Within the samples, special attention was paid to the region with co-existing $\alpha(O)+\beta$ phases. This region is not homogenous and considering 1D diffusion modeling, a special data treatment has to be performed to compare experimental data to modeling results. Using EPMA measurements, oxygen distribution within the cladding samples after steam oxidation was better characterized. Average radial profiles of oxygen have been determined assuming that the phase contents are uniform and close to equilibrium conditions. The oxygen profile is compared to diffusion simulations using the DIFFOX tool. The model prediction has shown that oxygen diffusion in the mixed phase region has to be improved. A new modeling was consequently proposed to determine the oxygen diffusion mechanisms in the two-phase region. The modeling results are satisfactorily compared to a large set of experiments. This model has been only fitted and validated at 1200°C and should be further tested at other oxidation temperatures.

5. References

- [1] H.M. Chung, T.F. Kassner, "Pseudobinary Zircaloy-Oxygen phase diagram ", Journal of Nuclear Materials 84, pp. 327-339, (1979).
- [2] J.-C. Brachet et al, "Hydrogen content, peroxidation, and cooling scenario effects on post-quench microstructure and mechanical properties of Zircaloy-4 and M5® alloys in LOCA conditions", Journal of ASTM International, Vol.5, n°5, Paper ID JAI101116, (2008).
- [3] J.C. Brachet et al, "Influence of hydrogen content on the α/β phase transformation and on the thermal-mechanical behavior of Zy-4, M4 and M5 alloys during the first phase of LOCA transient", Zirconium in the Nuclear Industry: 13th International Symposium, ASTM-STP 1423, pp. 673-701, Annecy, France, (2001).
- [4] N. Waeckel, "Fuel Safety Research at EDF", FSRM Meeting, Tokyo, (2005).
- [5] M. Billone, Y. Yan, T. Burtseva, R. Daum, "Cladding embrittlement during postulated Loss-of-Coolant Accidents", NUREG-CR-6967, US-NRC, (2008).
- [6] A. Sawatsky, "A proposed criterion for the oxygen embrittlement of Zircaloy-4 fuel cladding", Zirconium in the Nuclear Industry: 4th International Symposium, ASTM STP 681, pp. 479-496, (1979).
- [7] H.M. Chung, A.M. Garde, T.F. Kassner, "Mechanical properties of Zircaloy containing oxygen", ANL-77-10, Argonne National Laboratory, (1976).
- [8] E. Torres, J. Desquines, M-C. Baietto, M. Coret, F. Wehling, M. Blat-Yrieix, A. Ambard, "Adsorption and diffusion of hydrogen in Zircaloy-4", Fontevraud 8 - Contribution of Materials Investigations and Operating Experience to LWRs' Safety, Performance and Reliability, paper 198-T09-FP, (2014).
- [9] X. Ma, C. Toffolon-Masclet, T. Guilbert, D. Hamon, J.C. Brachet, "Oxidation kinetics and oxygen diffusion in low-tin Zircaloy-4 up to 1523K", Journal of Nuclear Materials 377, pp. 359-369, (2008).
- [10] C. Duriez et al, "Characterization of Oxygen Distribution in LOCA Situations", Journal of ASTM International, Vol. 8, No. 2 (2010).
- [11] E. Torres, J. Desquines, S. Guilbert, M-C. Baietto, M. Coret, P. Berger, M. Blat-Yrieix, A. Ambard, "Hydrogen motion in Zircaloy-4 cladding during a LOCA transient", Ic-cmtp3 international conference (2014).
- [12] J.V. Cathcart, R.E. Pawel, R.A. McKee, R.E. Druschel, G.J. Yurek, J.J. Campbell, S.H. Jury, "Zirconium metal-water oxidation kinetics IV. Reaction rate studies", NRC report ORNL/NUREG-17 (1977).
- [13] S. Guilbert, C. Duriez, C. Grandjean, "Influence of a pre-oxide layer on oxygen diffusion and on postquench mechanical properties of Zircaloy-4 after steam oxidation at 900°C", Proceedings of 2010 LWR Fuel Performance/TopFuel/WRFP, Orlando, Florida, USA, September 26-29, 2010 - Paper 121 (2010).
- [14] S. Guilbert et al, C. Grandjean, "Effect of Pre-oxide on Zircaloy-4 high-temperature steam oxidation and post-quench mechanical properties", ASTM STP 1523 (2013).
- [15] C. Raepsaet, P. Bossis, D. Hamon, J.L. Béchade, J.C. Brachet, "Quantification and local distribution of hydrogen within Zircaloy-4 PWR nuclear fuel cladding tubes at the nuclear microprobe of the Pierre Süe Laboratory from μ -ERDA", Nuclear Instruments and Methods in Physics Research section B, Vol. 266 pp. 2424–2428, (2008).
- [16] J.C. Brachet et al, "Oxygen, hydrogen and main alloying chemical elements partitioning upon alpha-beta phase transformation in zirconium alloys", Solid State Phenomena Vols.172-174, pp 753-759, (2011).
- [17] M. Le Saux et al, "Influence of pre-transient oxide on LOCA high temperature steam oxidation and postquench mechanical properties of Zircaloy-4 and M5™ cladding", Water Reactor Fuel Performance Meeting, paper T3-040, (2011).
- [18] C. Desgranges, C. Toffolon-Masclet et al., "Simulation of Oxygen diffusion during high temperature oxidation of Zr base Alloys", Solid State Phenomena Vols.172-174, (2011).
- [19] J.C. Brachet et al., "Mechanical behavior at Room Temperature and Metallurgical study of low-Tin Zy-4 and M5™ after oxidation at 1100°C and quenching", Proc. of TCM on "Fuel behavior under transient and LOCA conditions", IAEA, Halden-Norway, Sept. 10-14, (2001).
- [20] J.Crank - The mathematics of diffusion - Oxford University Press, (1956).
- [21] R.A. Perkins, "Oxygen diffusion in β -Zircaloy", JNM vol 68, pp.148-160, (1977).